Resonance Phenomena of Log-Periodic Antennas: Characteristic-Mode Analysis

MARTIN HILBERT, MARK A. TILSTON, AND KEITH G. BALMAIN, FELLOW, IEEE

Abstract—**The method of characteristic modes is implemented in the form of a general-purpose computer program based on an established moment-method program using piecewise sinusoids. Application of the method to the log-periodic dipole antenna (LPDA) yields characteristic modes that are insensitive to changes in moment-method segmentation and are revealing with regard to parasitic resonance phenomena. The study of the modes on LPDAs shows that the asymmetry resonance is dominated by a mode that is not restricted to one cell, although the single-resonant-cell postulate remains a good first-order explanation. On the other hand, the symmetric termination resonance is shown to involve more than one mode. A numerical study of various antenna deformations shows that only length extensions cause strong asymmetry resonances. The *E*-plane array is analyzed, and the results are shown to compare favorably with experiment.**

I. Introduction

THE LOG-PERIODIC dipole antenna (LPDA) is a popular choice for systems requiring a constant radiation pattern and input impedance over a wide frequency band. However, under certain conditions, narrow-band parasitic resonances that degrade antenna performance are known to occur [1]–[3]. These resonances are of two types, both involving the feeder line which extends from the feed point at the small end of the antenna to a short-circuit termination just beyond the large end of the antenna. One type of resonance involves feeder energy leaking past the radiating region and exciting a resonance between the short-circuit termination and the dipole that is closest to a half-wavelength. This resonance results in an altered current distribution that produces a decrease in the front-to-back ratio, and this resonance occurs when the half-wave dipole is separated from the termination by an odd number of loaded-transmission-line half-wavelengths. This resonance is called a *termination resonance* because it involves the flow of high currents in the short-circuit termination and is therefore highly dependent on both the termination position and the termination impedance. The termination resonance may be eliminated either by the insertion of lossy material in the termination region, or by the replacement of the short circuit with a matched resistor. It may be reduced by the use of thicker dipoles as the radiating elements [4].

The other type of resonance is known as an *asymmetry resonance* because it always occurs on LPDAs having physical asymmetry [3]. It also occurs whenever two or more LPDAs are configured as an *E*-plane array even though each of the individual antennas may be free from structural asymmetries [1]. It is interesting to note that this resonance can be excited even on a single, symmetric LPDA by incoming waves propagating in a wide range of off-boresight directions, but under these conditions, the resonance will not couple to the antenna terminals.

The asymmetry resonance involves a net current flowing on the transmission-line feeder (boom). Clearly, this could never happen in the case of a symmetric LPDA being used as a transmitting antenna because ideally the excitation would be symmetric, with the result that the currents on each of the two wires comprising the boom would be equal and opposite. However, the asymmetry resonance is excited whenever asymmetries are present. The net feeder current is responsible for the radiation to the side which always accompanies this resonance. Furthermore, the region on the feeder where the net current is strongest seems to be localized and is in the vicinity of the radiating region. Thus, an early explanation of the phenomenon was the *resonant cell postulate* of Balmain and Nkeng [3], depicted in Fig. 1. The asymmetry resonances also affect the antenna input impedance, causing small loops to appear in a swept-frequency Smith chart display [3].

Some theoretical work has been done on both the termination resonance [2] and the asymmetry resonance caused by the change in length of one monopole on the LPDA [5]. The latter work includes an investigation of the resonant cell postulate: a parallel-wire resonator was analyzed as it was deformed into the shape of a LPDA cell. The present work is a theoretical investigation of the LPDA both with and without physical asymmetries. The *E*-plane array is also considered and the theoretical results pertaining to it are compared with experimental data [6]. The method of characteristic modes [7], [8] is used in this analysis in the expectation that the breaking up of the current into basis functions particular to the antenna might provide new insight into the resonance phenomena and also might provide suggestions as to how to reduce the unwanted resonances.

II. Characteristic Mode Theory

Exact solutions for current flow exist for certain structures whose boundaries coincide with coordinate surfaces of coordi-

Manuscript received August 11, 1987; revised June 30, 1988. This work was supported by the Natural Sciences and Engineering Research Council of Canada Operating Grant A-4140.

M. Hilbert was with the Department of Electrical Engineering, University of Toronto, Toronto, Canada M5S 1A4. He is now with The Oratoru of St. Philip Neri, Toronto, ON, Canada.

M. A. Tilston was with the Department of Electrical Engineering, University of Toronto, Toronto, ON, Canada. He is now with M. A. Tilston Engineering, 90 Lawrence Avenue East, Toronto, ON, Canada M4N 1S6.

K. G. Balmain is with the Department of Electrical Engineering, University of Toronto, Toronto, ON, Canada M5S 1A4.

IEEE Log Number 8929256.

0018-926X/89/1000-1224$01.00

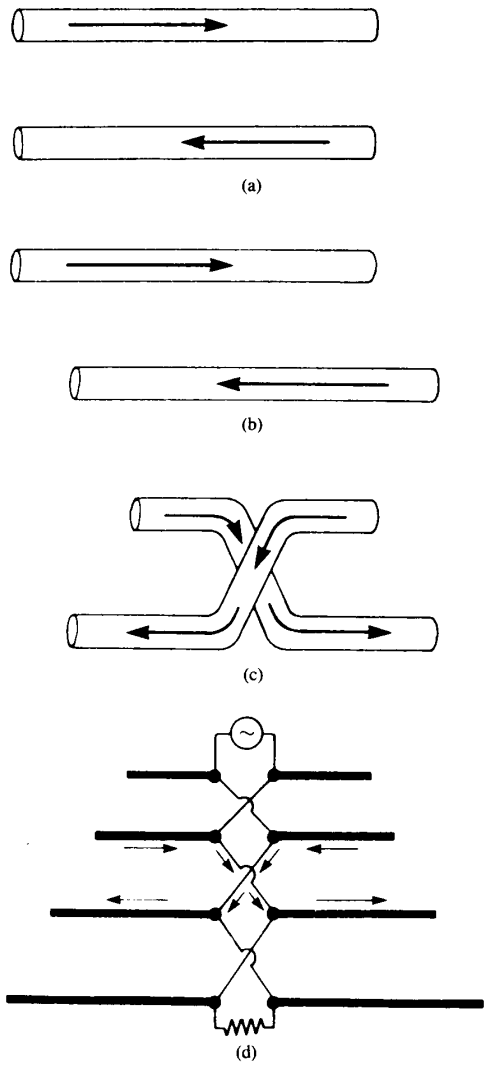

Fig. 1. The "resonant cell postulate" of Balmain and Nkeng [3]. (a) Parallel wire resonator is (b) offset, (c) bent, and (d) incorporated into a log-periodic dipole antenna.

nate systems in which the Helmholtz equation is separable. The solutions are summations of infinite sets of basis functions. Garbacz [7] has shown that it is possible to determine numerically a set of basis functions for the current on an arbitrary conducting body. The following outlines the numerical solution and lists some of the properties of the resulting basis functions or characteristic modes, following Harrington and Mautz [8].

Starting with a symmetric mutual impedance matrix $Z = R + jX$ computed by a moment-method program, a weighted eigenvalue equation is set up,

$$XI_n = \lambda_n R I_n. \tag{1}$$

The resulting eigenvectors I_n are the characteristic modes, and λ_n are the corresponding eigenvalues. The subscript n ranges in value from one to the order of the matrix. Because the Z matrix is symmetric, the eigenvalues, and hence the eigenvectors (characteristic modes), are real. Also, owing to the symmetry of Z, certain orthogonality conditions hold. With suitable normalization, the following are true:

$$I_m^T R I_n = \delta_{mn}$$
$$I_m^T X I_n = \lambda_n \delta_{mn}$$
$$I_m^T Z I_n = (1 + j\lambda_n)\delta_{mn} \tag{2}$$

in which δ is the Kronecker delta, m and n are integers, and T denotes transpose. The far fields of the modes may be shown to be orthogonal also. Thus each mode radiates power independent of the other modes. It may also be shown that the sign of the eigenvalue is determined by the type of stored energy that is dominant for each characteristic current. If the magnetic stored energy dominates, the eigenvalue is positive and may be termed inductive; if electric, then the eigenvalue is negative and capacitive. Note that resonance corresponds to $\lambda_n = 0$.

Finally, if V is understood to be the voltage vector as encountered in a moment-method equation $ZI = V$, then the total current flow I_t is given by

$$I_t = \sum_{n=1}^{N} \frac{I_n^T V}{1 + j\lambda_n} I_n. \tag{3}$$

Modes with small eigenvalues, and thus closer to resonance, are easier to excite. The location of the voltage source is also important because, if the feed point is located at a characteristic current null, then that mode will not be excited.

In practice, it was found that only a few modes contribute to the total current flow on an LPDA. If the modes are ordered in ascending values of $|\lambda_n|$, it is only the lower-order modes that need be used in the summation. Although it was found that the normalized modal currents were greater for higher order modes, the increase was slight in comparison to the increase in $|\lambda_n|$ and thus the higher order modes contributed only a negligible current (equation (3)).

In the present work, a moment-method program due to J. H. Richmond, based on Galerkin's method and piecewise sinusoids [9], was used to generate the mutual impedance matrix Z. Commercially available software was then used to solve the eigenvector problem [10]. As a test of the accuracy of the characteristic-mode computation, the LPDA input impedance determined in this way was compared with the input impedance determined by matrix inversion of the system $ZI = V$; the agreement was to three significant digits. Richmond's moment-method program forces the Z matrix to be symmetric, so the eigenvalues turn out to be real as expected, but computational inaccuracy can still produce incorrect eigenvalues and eigenvectors. Therefore, as a further test of computational accuracy, the first of equations (2) was computed for each characteristic mode and some discrepancies were noted, but only for three or four of the highest eigenvalues for which the contribution to the complete solution is entirely negligible.

Since any moment-method program requires a segmentation of the structure under consideration, the modes were tested to

determine their sensitivity to the segmentation scheme. Although a small discrepancy was found in the eigenvalues, the characteristic currents remained unaltered to any appreciable extent. The characteristic modes were also insensitive to changes in the calculation of the mutual impedance matrix. The changes referred to were those required to eliminate the so-called "computer-generated asymmetries" reported by Vainberg and Balmain [5] and to eliminate changes in the moment-method solution due to the renumbering of a given segmentation scheme. These modifications to Richmond's program (due primarily to one of the authors, M. A. T.) are presented in the Appendix. In addition, application of the characteristic-mode method to simple structures such as transmission line resonators and simple dipole antennas produced current flows and input impedances in agreement with known results.

III. Antennas Used in Study

The primary antenna used in the numerical simulation was a typical nine-element LPDA with $\tau = 0.89$, $\sigma = 0.15$ and a frequency range of 600 to 850 MHz: the longest dipole was 25 cm long, tip-to-tip. The characteristic transmission-line impedance of the feeder was 135 Ω, a value high enough to avoid significant error arising from the "thin wire" assumption employed in Richmond's program. The feeder was terminated with a short circuit 6.25 cm beyond the longest dipole. The feeder used in this study comprises a pair of straight cylindrical conductors equivalent to the "criss-cross" configuration employed for conceptual clarity in Fig. 1. Most results presented assumed a wire conductivity of 10 MS/m and a wire radius of 1 mm. Changing the wire radius, although not significantly affecting the resonance behavior, does shift the resonance frequencies. For a 1 mm radius, the asymmetry resonances were at 573, 667, and 779 MHz, and a termination resonance was at 811 MHz. For the case of a 3 mm radius, the 779 MHz asymmetry resonance was shifted upward to 810 MHz and the 811 MHz termination resonance upward to 837 MHz. In comparison with thicker wires, the computations showed that thinner wires cause larger performance degradations at termination-resonance frequencies and smaller performance degradations at asymmetry-resonance frequencies. Exact comparison with experiment is impossible since the program in the form used cannot handle segments of different wire radii and the actual antennas used were made of two different wire thicknesses (boom radius = 3.2 mm, monopole radius = 1.5 mm).

Also considered was a highly compressed seven-dipole LPDA with $\tau = 0.89$, $\sigma = 0.019$, and a frequency range from 550 to 740 MHz. The feeder characteristic impedance was 100 Ω. This was not meant to be an example of a good antenna but rather as a test of the resonant cell postulate; this was the only antenna investigated by Balmain and Nkeng [3] that had the same number of asymmetry resonances as cells.

IV. Characteristic Modes on a Symmetric Antenna

By symmetry, it is evident that only two types of modes can exist on a symmetric LPDA. The first type has equal and opposite currents everywhere on the transmission-line feeder

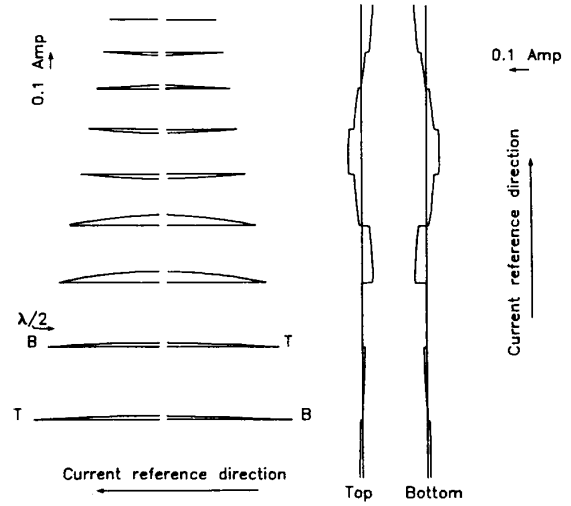

Fig. 2. The dominant radiating symmetric mode at 700 MHz. The arrow indicates the location of the λ/2 dipole. The current reference directions and the scale are indicated on this graph. Subsequent graphs have only one scale arrow and no reference direction arrows. The antenna itself is drawn to scale. The designations T and B indicate that the associated monopoles are attached to the "top" and "bottom" feeder wires, respectively. At the large end of the antenna, the two feeder wires are terminated with a short circuit.

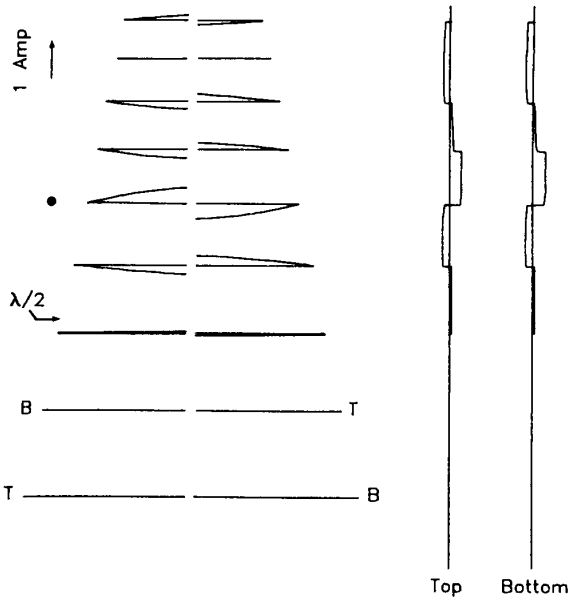

Fig. 3. The dominant resonant asymmetric mode at 779 MHz, an asymmetry resonance frequency. The dot indicates monopole #5t which is elongated in the study of asymmetries.

and symmetric currents on opposing monopoles (see example in Fig. 2: note that this figure and all subsequent figures present *computed* results). Since modes of this type are responsible for radiation under symmetric excitation, they will be referred to as *radiating symmetric*. The second type of mode has equal and co-directional currents everywhere on the transmission-line feeder and equal and opposite currents on opposing monopoles (Fig. 3). This type of mode is responsible

for the asymmetry resonances and will thus be termed *resonant asymmetric*.

Before discussing some of the specifics of these modes, it is instructive to recall that the contribution of each mode to the total current is directly proportional to the modal current at the point of excitation and inversely proportional to $1 + j\lambda_n$ where λ_n is the associated eigenvalue. The modes are hence numbered in ascending values of $|\lambda_n|$. Of the 110 modes associated with the standard antenna, usually the first five or six have an eigenvalue of 10 or less, and the next two or three have an eigenvalue between 10 and 100. After that, the contributions of the modes become insignificant. The largest eigenvalues are of the order of a million.

When excited by a feed-point source located halfway between the two feeder wires, the antenna exhibits a traveling wave from the feed point to the radiating region, a condition requiring phase progression. Because characteristic modes are equiphase, it is expected that at least two modes will contribute strongly to the total current. An examination of the first three modes at 700 MHz, a nonresonant frequency, reveals this to be correct. These modes contribute 50, 28, and 16.5 percent of the total radiated power, with current phases of 3°, 113°, and 69° with respect to the input voltage. As the frequency is increased, more modes contribute significant percentages of the total power.

For the mode shown in Fig. 2, although the region of greatest modal current coincides with the radiating region, there is a nonnegligible current flow in the termination region (i.e., the region between the half-wave dipole and the feeder short-circuit). This is true also of the other radiating symmetric modes that contribute significant percentages of the total radiated energy. However, the total current, determined by summation of the individual modes (equation (3)), has negligible components beyond the radiating region, except at termination resonance frequencies. Note on Fig. 2 and subsequent figures that the indicated "λ/2 dipole" is actually the location where the envelope of dipole end points is λ/2 wide, and the "radiating region" is generally the next smaller three or four dipoles.

Before discussing the resonant asymmetric modes and their associated Q values, it is necessary to consider how much the characteristic modes change from one frequency to another. In most cases the change is small enough and the modes are distinct enough that it is possible to associate the modes from a solution set at one frequency with those from a solution set at a different frequency just by visual inspection of the currents. However, cases do arise where this is not possible. Nevertheless, it is possible to associate the modes by plotting their eigenvalues as a function of frequency. This was found to produce a smooth curve in all cases attempted and hence is a good method of sorting the modes [11].

Fig. 3 shows a resonant asymmetric mode at 779 MHz, an asymmetry resonance frequency. This mode has a maximum of current along the transmission-line feeder between the dipoles carrying the most current. Since its eigenvalue is very close to zero at this frequency, it is the first mode in the solution set. It also has the largest current flow of the low-order resonant asymmetric modes and is the only low-order

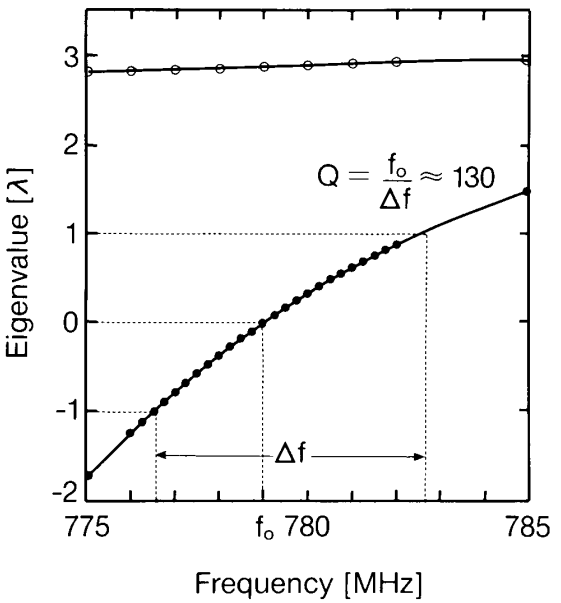

Fig. 4. A plot of eigenvalues showing how one deduces the quality factor Q of the resonant asymmetric mode of Fig. 3 (indicated by dots). The top curve (indicated by circles) shows eigenvalues for the second most dominant resonant asymmetric mode and is included to show that this mode does not contribute to the resonance.

resonant asymmetric mode whose eigenvalue varies rapidly with frequency (Fig. 4). Hence, the quality factor Q associated with this mode will be essentially the Q associated with the total current flow in any experiment designed to detect an asymmetry resonance around this frequency. Since the excitation is inversely proportional to $1 + j\lambda_n$, it follows that the 3 dB frequencies correspond to $\lambda_n = \pm 1$ (given that the actual modal current does not change significantly over the frequency band in question, as in fact it did not). With reference to Fig. 4, a value of $Q = 130$ was calculated for this mode which is approximately double the value estimated from the experimental results reported by Balmain and Nkeng [3]. Asymmetry resonances accompany zero crossings of the eigenvalue of this mode. At each higher resonant frequency, the mode is shifted one cell toward the apex of the LPDA. Thus, it always coincides with the radiating region. Because of this, any attempts to suppress the resonant asymmetric mode while leaving the radiating symmetric modes unaltered would be very difficult.

Although it bears a strong resemblance to the resonant cell postulate, the mode of Fig. 3 is not confined to one cell. A search of all the modes at an asymmetry resonance frequency failed to produce a mode that would fit the resonant cell postulate exactly. Despite this, the postulate remains a good first-order explanation of the asymmetry resonance phenomenon.

Because the resonant asymmetric modes all have a current null at the feed point, they are not excited by a transmitter. In the case of a receiving antenna and for the same reason, a wave incident from the side can excite the resonance, but it will not couple into the receiver.

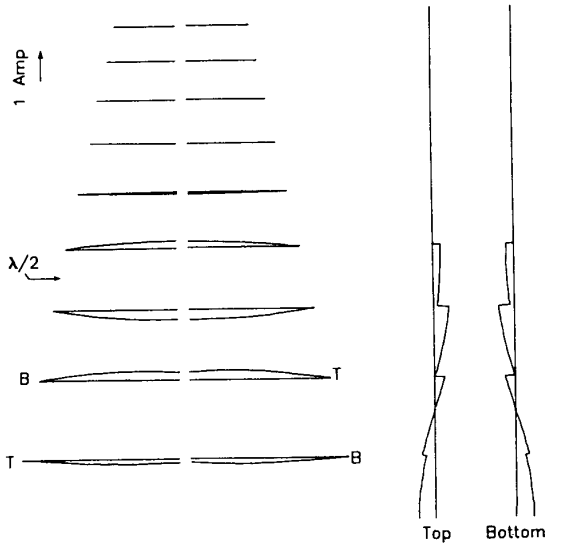

Fig. 5. The mode corresponding to the termination resonance as postulated by Bantin and Balmain [2]. The frequency is 811 MHz. This mode is eliminated upon replacement of the short circuit in the termination with a resistor.

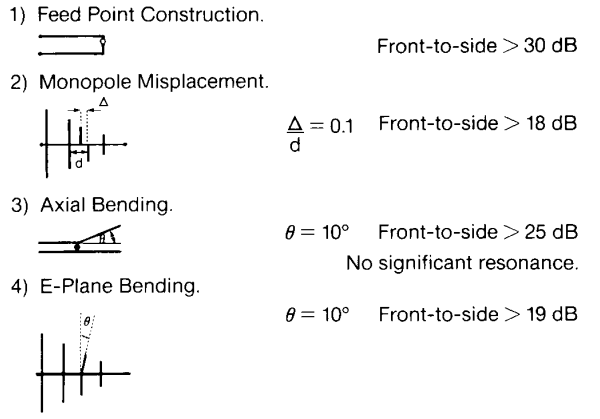

Fig. 6. Summary of antenna deformations studied. Note that, in (1), the feed point asymmetry was simulated by placing the voltage source right at one of the wires of the feeder boom rather than in the middle.

The termination resonance occurred at 811 MHz. An anomalous radiating region behind the primary radiating region, as reported by Gong and Balmain [4], was found by computation. When a matched resistor in the location of the transmission-line short-circuit termination was specified in the computer program, the anomalous radiating region was eliminated, as in [4]. With no resistor specified, a mode, which matches the description of the termination resonance given by Bantin and Balmain [2], was computed. A half-wave resonance between the short circuit termination and the dipole closest to a half-wavelength can be seen clearly in Fig. 5. This mode disappears from the solution set when a matched termination is specified.

Yet, the termination resonance is much more complicated than the above seems to suggest. With a short circuit termination, several modes with large current flows exist behind the radiating region. This in itself is not surprising since the phenomenon is observed at other frequencies. What is surprising is that, whereas at other frequencies the modal currents behind the radiating region cancel upon summation, at the termination resonance frequency they do not. Furthermore although the total current behind the radiating region is very similar to the mode of Fig. 5, at least three other modes contribute significantly to it. When a matched termination is specified, several modes still exhibit large current flows in the termination region. However, they are modified such that, upon summation, the anomalous radiating region is eliminated; and, as mentioned above, the mode of Fig. 5 is not found in the solution set at all.

Calculations were performed on a compressed antenna with the hope that a mode that would more closely resemble the resonant-cell postulate might be found. It was thought that the compressed radiating region would prevent current flows on any dipoles that were outside the resonant cell. The results proved that this is not the case: the dominant asymmetric mode around resonance, while strongly resembling the resonant-cell postulate, was still not restricted to one cell.

V. Asymmetry Conditions

Several structural asymmetries were studied to determine the relative severity of the antenna performance degradation caused by each. Of the five structural deformations considered, only one, monopole extension, caused strong resonances. Fig. 6 summarizes the four asymmetries that produced relatively minor sidelobe levels despite the rather large structural deformations, all of which could be detected and corrected from observation by the unaided eye.

Monopole extension causes the strongest resonances. In the numerical study of the standard antenna, monopole #5t, indicated by a dot in Fig. 3, was extended by varying amounts. This monopole was chosen because it is in the middle of the antenna and hence should be shielded from end effects. It is a quarter wavelength at 956.3 MHz.

Fig. 7 displays results obtained by matrix inversion (and confirmed by the eigenvector solution), showing the E-plane front, side, and back lobe gain as a function of frequency for the case of 5 and 12.4 percent monopole extension. The 12.4 percent case corresponds to $(\tau^{-1}-1)\times 100$ percent, and thus was used to simulate the effect of an assembly worker erroneously attaching two monopoles of the same length onto the boom at different locations.

Even though there are increases in sidelobe levels around 572 and 667 MHz due to asymmetry resonances, the effect is much smaller than at 779 MHz. This is because monopole #5t was not part of the radiating region at the lower frequencies. Extensions of 1, 2, 5, and 12.4 percent failed to change the resonance frequency around 667 MHz by more than 0.5 MHz. This suggests that the element is not directly involved in the resonance but rather serves only to excite it.

At 779 MHz monopole #5t supports a large current flow on a symmetric antenna. Fig. 8 shows the change in resonant frequency as a function of percentage monopole extension. The linear graph indicates that the resonance strongly depends on the length of monopole #5t which suggests that the

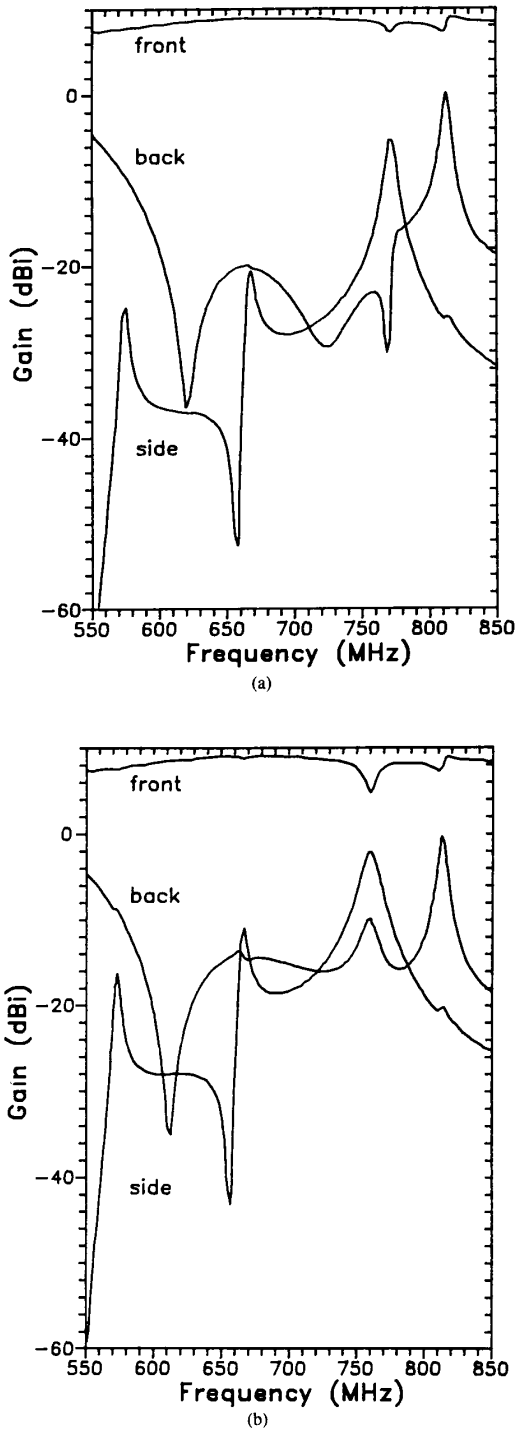

Fig. 7. Gain versus frequency for two cases of extension of monopole #5t. Note that only the resonance around 770 MHz has its frequency changed with the amount of extension. The peak in the back lobe level at 811 MHz is due to the termination resonance. (a) 5 percent extension. (b) 12.4 percent extension.

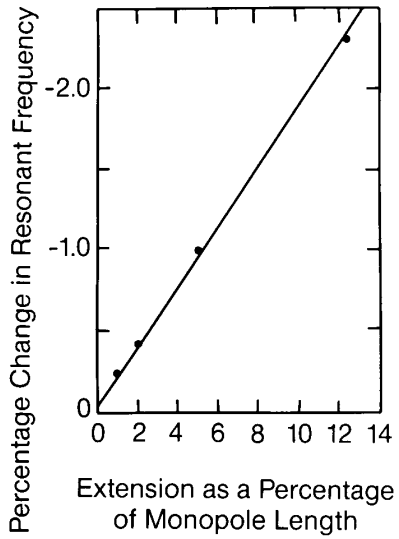

Fig. 8. Percentage change in resonant frequency versus percentage extension of monopole #5t.

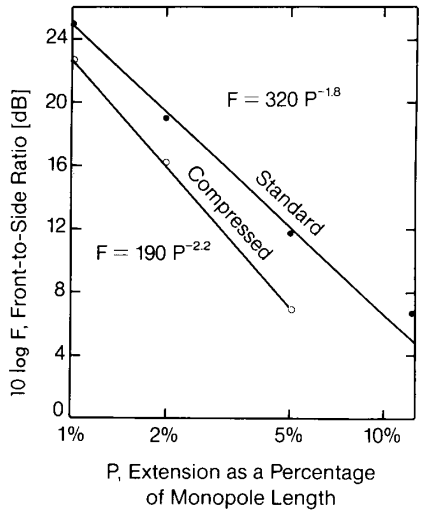

Fig. 9. The front-to-side power ratio as a function of the percentage extension on a log scale.

monopole is integral to the resonance. A 10 percent change in monopole length, however, results in only a 2 percent change in resonant frequency, suggesting that the resonance must extend over more than one cell.

The front-to-side ratio as a function of percentage monopole extension for both the standard and compressed antennas is shown in Fig. 9. The linear graph on a log-log plot suggests that a simple power law relation must hold for the front-to-side power ratio, F as a function of percentage extension P. It is

$$F = 320P^{-1.8} \tag{4}$$

for the standard antenna and

$$F = 190P^{-2.2} \tag{5}$$

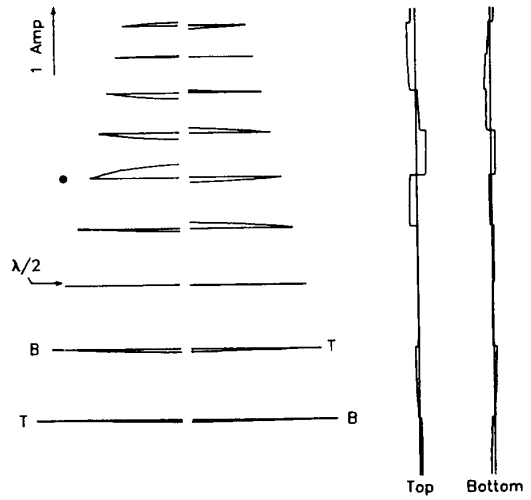

Fig. 10. Mode two on antenna with monopole #5t extended 12.4 percent at 761 MHz, an asymmetry resonance frequency. This is a remnant of a radiating symmetric mode as may be determined by a series of small distortions or by considering the current near the termination, far removed from the radiating region.

for the compressed antenna. The formula for the standard antenna yields a front-to-side ratio 5 dB lower than experimentally derived by Balmain and Nkeng [3]. The discrepancy probably comes from an inability to simulate two different wire thicknesses.

The asymmetric component of the total current distribution at an asymmetry resonance frequency was computed. This component is the unbalanced current on the transmission-line feeder together with the oppositely directed currents on the dipoles. Given all the total currents, their asymmetric components can be found readily, for example by calculating the sum of the two boom currents and dividing this net current equally between the two booms. While many modes contributed to these asymmetric current components, the result very much resembles the resonant asymmetric mode of Fig. 3. It is this mode that was shown to be responsible for the high-Q resonances.

The modes on one antenna that has had one of its monopoles extended are neither resonant asymmetric nor radiating symmetric but rather hybrids of the two types (Fig. 10). Nevertheless, it is often possible to identify corresponding modes on a symmetric antenna just by visual observation of the currents. Sometimes, however, the hybrids are so distorted that the only way to determine their origin is to perform a series of computations with increasingly large distortions. Examination of the current far removed from the distortion region or the radiating region may also be useful in identifying the origin of the modes.

A few general rules seem to hold for modes on a distorted antenna. Modes that had little current on the symmetric antenna on the monopole that was subsequently extended were not substantially changed by the elongation, but the inverse of this statement is not generally true. The higher order modes were affected less by an extension than were the lower order modes. At asymmetry resonance frequencies, resonant asymmetric modes were distorted less than radiating symmetric modes. Conversely, at frequencies removed from asymmetry resonance, it is the set of radiating symmetric modes that remained intact.

A 12.4 percent extension of monopole #5t caused a maximum in sidelobe level at 761 MHz. A study of the eigenvalues on this distorted antenna as the frequency varied from 758 to 762 MHz revealed that no mode has a small eigenvalue that varied quickly with frequency. Rather, the narrow resonance was caused by the distortion of one mode near the feed point. This, of course, has a strong effect on the modal excitation coefficient.

VI. E-Plane Array

Log-periodic dipole antennas have been successfully used in H-plane arrays for a number of years [12]. This configuration was used to narrow the H-plane beamwidth which is wider than the E-plane beamwidth on a single antenna. Further attempts to increase gain by using an E-plane array (Fig. 11(a)), however, have revealed serious performance degradations in narrow frequency bands [1]. A decrease in front-lobe gain accompanied by an increase in radiation to the side and high SWR, all encountered in the case of an imperfectly constructed antenna, are found as well with the E-plane array, no matter how carefully the array and each of its component antennas are constructed.

To maintain frequency-independent operation for an array, it is necessary to place the antennas in the common-apex configuration of Fig. 11(a). This keeps a constant separation in terms of wavelengths between the radiating regions of the two antennas. The performance of the array is dependent on the angle δ between the antenna axes. Experimental results [6] are available, and will be presented here together with numerical results, for array angles 25° and 30°. For the antennas used, the minimum possible angle that would prevent overlap is 20.8°.

The asymmetry resonances are very pronounced, in both the experiments and the computations, due to the strong asymmetric couplng between the dipoles on one antenna and the feeder on the other. As in the case of the single antenna, the wire radius specified had an effect on the computed results. Thinner wires lowered the frequency of both the asymmetry resonance and the termination resonance. Thinner wires also produced higher front-to-side ratios at asymmetry resonances and lower front-to-back ratios at termination resonances. These are the same trends as were exhibited in the computations involving a single antenna.

The best agreement between theory and experiment was obtained when the theoretical wire diameter was 3 mm, slightly less than the 3.2 mm diameter of the wire used to construct the booms of the antennas used in the experiment. Table I shows the asymmetry resonance frequencies and the accompanying front-to-side ratios determined both computationally and experimentally. Note that "front" refers to the array boresight axis and "side" refers to the direction at 90° from boresight and lying in the E-plane (the plane of the array). Similarly the "back" lobe is in the direction at 180° from array boresight.

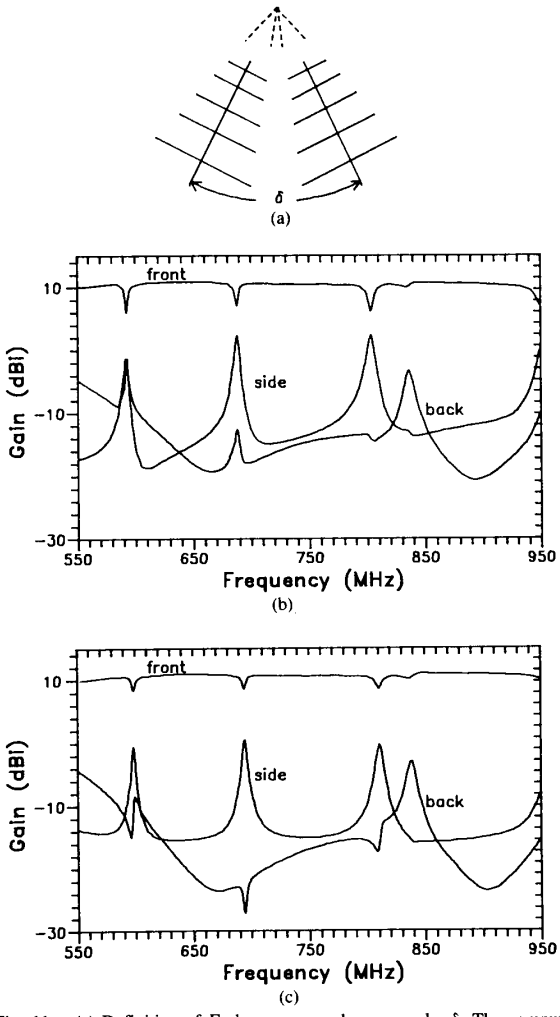

Fig. 11. (a) Definition of *E*-plane array and array angle, δ. The computed front, side, and back lobe gain are shown for (b) $\delta = 25°$ and (c) $\delta = 30°$. Wire radius is 3 mm.

TABLE I
RESONANCE FREQUENCY/FRONT-TO-SIDE RATIO

$\delta = 25°$		$\delta = 30°$	
Computation	Experiment	Computation	Experiment
592 MHz/6.8 dB	593 MHz/2 dB	598 MHz/9.0 dB	602 MHz/ 7.1 dB
688 MHz/4.6 dB	692 MHz/5 dB	694 MHz/8.3 dB	697 MHz/ 9.8 dB
804 MHz/3.7 dB	804 MHz/3 dB	811 MHz/8.8 dB	810 MHz/10.5 dB

The experimental results were judged accurate to ± 1 dB. A different segmentation scheme was used to check the accuracy of the numerical results. This shifted the 688 MHz resonance to 686 MHz and changed the accompanying front-to-side ratio from 4.6 to 4.9 dB. It is interesting to note that the asymmetry resonance frequency increases with increasing array angle. If higher front-lobe gain, which is slightly higher for the larger array angle, and higher front-to-side ratio at resonance are used as criteria, the larger angle is clearly better. This is probably due to less coupling between the adjacent antenna cells.

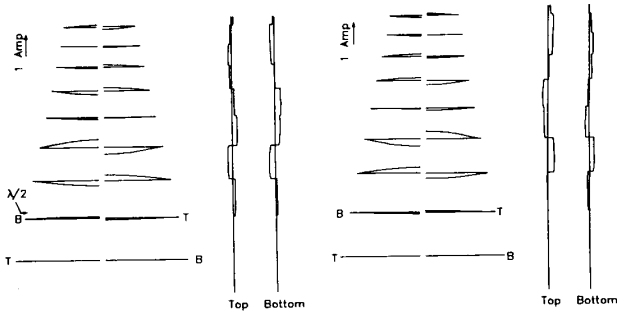

Fig. 12. *E*-plane array mode that radiates under in-phase excitation a significant percentage of the total power at 688 MHz, an asymmetry resonance frequency. Note that the current on each antenna resembles the resonant asymmetric mode. Angle $\delta = 25°$.

The termination resonance present on an antenna array manifests itself by an increase in back-lobe gain. It is not dependent on the array angle for its actual frequency or the resulting front-to-back ratio. However, it is very dependent on the wire radius. A 1 mm wire caused dips in the computed front-lobe gain comparable to those caused by the asymmetry resonances. This was not the case with the thicker wire which produced smaller dips. For both wire radii, specification of a terminating resistor in the calculation suppressed the resonance. Fig. 11 shows the front, side, and back lobe gain as a function of frequency, summarizing most of the above mentioned points.

The modes on an array no longer possess symmetry about the top and bottom of each antenna as was the case for a single radiator. Symmetry, however, still exists from one antenna to the other, and again there are two types of modes. One type is excited if the two antennas are fed in-phase so as to produce a maximum of radiation in the direction of the apex. Out-of-phase voltage sources, as are used in radar applications to produce deep nulls in the boresight direction, excite the other type of mode.

At an asymmetry resonance frequency, under in-phase excitation, the modes that radiate significant percentages of the total radiated power resemble the resonant asymmetric modes on a single antenna (Fig. 12); off resonance, the modes resemble the radiating asymmetric modes.

VII. Conclusion

The method of characteristic modes produces antenna performance predictions that are in good agreement with those produced by standard moment-method programs. As an analytical method to find the current distribution, the method of characteristic modes is useful if a set of basis functions is desired rather than a particular solution. These basis functions are insensitive to changes in moment-method segmentation. Because only a few characteristic modes have small eigenvalues (hence large currents), even on an electrically large and complicated structure as is the LPDA, an understanding of antenna operation may be derived from these dominant modes only.

The modes on a perfectly constructed LPDA are either *radiating symmetric* or *resonant asymmetric*, and the resonant asymmetric modes are not excited on an ideal transmitting antenna because a properly designed feed point provides symmetric excitation. In the presence of physical asymmetry, the modes excited are hybrids of these two basic types, hybrids which resemble the basic types for small asymmetries; thus, it is approximately correct to assert that physical asymmetry results in the excitation of asymmetric characteristic modes. Because the dominant modes of either kind have large currents in the radiating region, to suppress the resonant asymmetric type without altering the radiating symmetric type and without destroying the frequency-independent nature of the antenna appears to be very difficult. For a single antenna, the only known method for reduction of asymmetry resonance excitation is increased construction accuracy, and this paper provides additional information on the kind and magnitude of accuracy required. The study of various antenna deformations shows that the LPDA performance is degraded most by asymmetries in dipole length. Other asymmetries, such as monopole bending, monopole misplacement and feed-point offset, cause relatively weak resonances, if any at all. In an E-plane array, modes that are hybrids between the two types of modes found on a single antenna are strongly excited; hence, the reduction of the asymmetry resonances is difficult and can be achieved only by increasing the separation between the component LPDAs in the array.

The *termination resonance* occurs on perfectly symmetric antennas having a short-circuit feeder termination at the large end of the antenna. This resonance emerges as a sum of characteristic modes, two of which penetrate into the normally unexcited large end of the antenna and one of which exists only in this region. When the short circuit is replaced with a matched feeder termination, the former two modes cancel each other and the latter mode vanishes. In an E-plane array, these properties of the termination resonance are the same as in a single antenna.

The computer program used is limited to a single conductor radius for the entire antenna although the experimental antennas referred to employed feeder conductors with a radius larger than the radius used for the dipoles. This discrepancy is deemed not to influence the conclusions reached because the computed modal current distributions were found to be independent of conductor radius over the range from the smaller to the larger of the two radii used in the experiments. Moreover, the best agreement between predicted and measured parasitic resonance frequencies occurred for a computational model with a conductor radius between the two experimental values, and the predicted and measured sidelobe levels at resonance frequencies were found to be comparable.

Appendix

As mentioned in the main body of the paper, there were some changes noted in the moment method solution of Richmond's program [9] when the segmentation was varied. Of importance was the unexpected change in the solution upon renumbering of segment endpoints. The renumbering problem was found to be due to the treatment of the computed mutual impedance matrix as being reciprocal, i.e., computing only the upper right triangular portion of the matrix (including the main diagonal) when, in fact, the mutual impedances as actually computed were not always reciprocal.

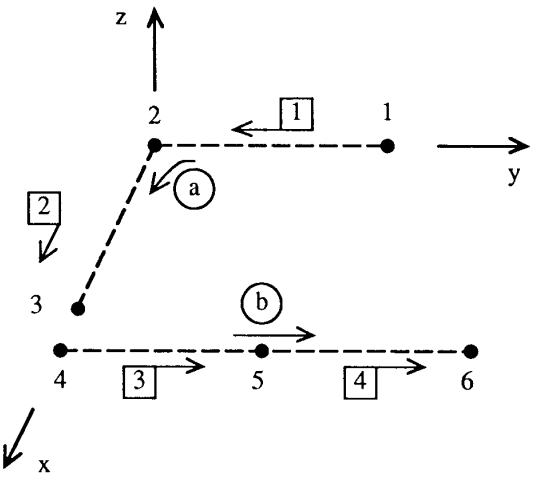

Fig. 13. Arrangement of segment axes for the example dipole-to-dipole mutual impedance problem. Boxed numbers denote monopoles, circled letters denote dipoles, and unenclosed numbers denote axis point numbers. Arrows indicate reference directions for current flow.

The problem of non-reciprocity was found to be caused by the way in which the mutual impedance between an expansion dipole and a testing dipole is computed. The dipole-to-dipole mutual impedance is computed as the sum of four filamentary monopole-to-monopole mutual impedances. Each monopole spans a wire segment. In a monopole-to-monopole mutual impedance computation, the two monopoles are placed on their respective segment axes unless the axes intersect or are coincident. If the axes are coincident, the monopoles are offset from one another by a wire radius in any direction orthogonal to the common axis. If the axes intersect, the monopoles are offset from one another by a wire radius in a direction orthogonal to the plane containing the two axes.

Consider a specific example of a dipole-to-dipole mutual impedance computation. Fig. 13 shows the configuration, with point numbers on the wire axes that define the span of the two dipoles and their four associated monopoles (two monopoles per dipole). The mutual impedance between the two dipoles is composed of four monopole-to-monopole impedances as follows:

$$Z_{ab} = Z_{13} + Z_{14} + Z_{23} + Z_{24}$$
$$Z_{ba} = Z_{31} + Z_{32} + Z_{41} + Z_{42}. \quad (6)$$

Of the above pairs of monopoles, those requiring an offset are: 2-3 and 2-4. Pairs 1-3 and 1-4 do not require an offset because their associated wire axes do not intersect. Fig. 14 shows a possible monopole geometry that satisfies the offset requirements. Note that monopoles 1 and 2 are offset relative to one another causing dipole a to be broken, while dipole b is continuous. To satisfy the continuity equation, there must be equal and opposite point charges on monopoles 1 and 2 at the dipole break. With the equation of continuity satisfied, the

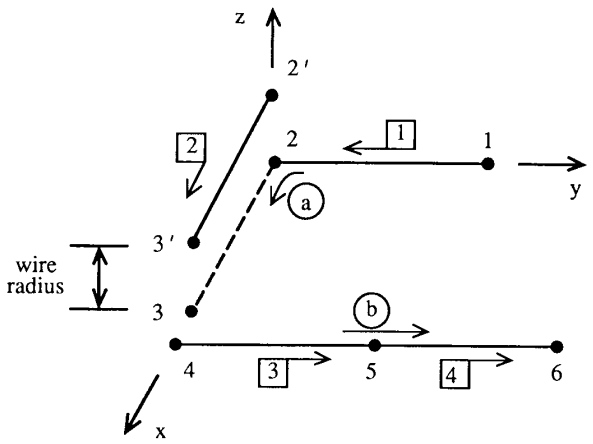

Fig. 14. Monopole locations for the example dipole-to-dipole mutual impedance computation.

mutual impedance between dipoles a and b is reciprocal. However, Richmond's program neglects the contribution to the E-field of the electric scalar potential gradient for the point charges when computing mutual impedance by using the following integral (where the current at the terminals is unity):

$$Z_{ab} = -\int \mathbf{E}_a \cdot \mathbf{J}_b \, dV. \tag{7}$$

Neglecting the point charges will affect $\mathbf{E}_a$ but not $\mathbf{E}_b$. Hence, Z_{ab} will be affected but not Z_{ba}, and reciprocity cannot hold.

To restore reciprocity to the broken dipole case, we modified the monopole-to-monopole mutual impedance computation to make it reciprocal. The modification involves including the point charges as follows: the point charge contribution to the mutual impedance is proportional to the integral of the point charge electric scalar potential gradient of one monopole dotted with the current of the other monopole. This was neglected in the original program. Integration by parts yields an equivalent integral which is the integral of the point charge electric scalar potential of one monopole multiplied by the charge (distributed charge plus point charge) of the other monopole. Only the point-to-distribution term of this integral was included. This involved modification of subroutine GGMM in the original program. The point-to-point term was not included because its contributions to Z_{ab} and Z_{ba} are the same, and therefore its inclusion is not necessary to bring reciprocity to the monopole-to-monopole mutual impedance.

The renumbering problem in Richmond's program not only caused slightly different solutions upon renumbering of points, but also caused apparent "computer-generated asymmetry" in a physically symmetric problem, as noted by Vainberg and Balmain [5] in their computation of E-plane side radiation from a symmetrical log-periodic dipole antenna. Any significant side radiation must come from asymmetry in the boom current. In the present work and before the program modification described above, it was found that with one particular numbering scheme there was no significant computer-generated asymmetry, while with other numbering schemes there was. The present modification yielded the same result for any numbering scheme (the same result, moreover, as from the original program using the numbering scheme that did not display incorrect asymmetry.)

References

[1] C. Elfving and S. Miller, "Gain variations in E-plane arrays of log-periodic antennas," Sylvania Electron. Syst. West, Mountain View, CA, Tech. Rep. ECOM-0503-P005-G815, Nov. 1969.

[2] C. C. Bantin and K. G. Balmain, "Study of compressed log-periodic dipole antennas," *IEEE Trans. Antennas Propagat.*, vol. AP-18, pp. 195-203, Mar. 1970.

[3] K. G. Balmain and J. N. Nkeng, "Asymmetry phenomenon of log-periodic dipole antennas," *IEEE Trans. Antennas Propagat.*, vol. AP-24, pp. 402-410, July 1976.

[4] Z. L. Gong and K. G. Balmain, "Reduction of the anomalous resonances of symmetric log-periodic dipole antennas," *IEEE Trans. Antennas Propagat.*, vol. AP-34, pp. 1404-1410, Dec. 1986.

[5] M. Vainberg and K. G. Balmain, "On prediction of the asymmetry resonance phenomenon of log-periodic dipole antennas," *Can. Elec. Eng. J.*, vol. 6, no. 3, pp. 31-34, 1981.

[6] A. Battagin, "E-plane array of log-periodic dipole antennas," B.A.Sc. thesis, Dept. Elec. Eng., Univ. Toronto, Toronto, ON, Canada, Apr. 1984.

[7] R. J. Garbacz, "A generalized expansion for radiated and scattered fields," Ph.D. dissertation, Ohio State Univ., Columbus, 1968.

[8] R. F. Harrington and J. R. Mautz, "Theory and computation of characteristic modes for conducting bodies," Sci. Rep. 9, Contract F19628-68-C-1080, AFCRL-70-0657, 1970.

[9] J. H. Richmond, "Computer program for thin wire structures in a homogeneous conductive medium," NASA CR-2399, June 1974.

[10] IMSL Library: FORTRAN Subroutines for Mathematics and Statistics, Edition 9.2, Nov. 1984, IMSL, LIB-0009, program EIGZF, IMSL, NBC Building, 7500 Bellaire Blvd., Houston, TX 77036.

[11] M. Hilbert, "Resonance phenomena of log-periodic antennas: characteristic-mode analysis," M.A.Sc. thesis, Dept. Elec. Eng., Univ. Toronto, Toronto, ON, Canada, Sept. 1985.

[12] R. H. Kyle, "Mutual coupling between log-periodic antennas," *IEEE Trans. Antennas Propagat.*, vol. AP-18, pp. 15-22, Jan. 1970.

Martin Hilbert was born in Prague, Czechoslovakia, in 1961. He received the B.A.Sc. degree in engineering science in 1983 and the M.A.Sc. degree in electrical engineering in 1985, both from the University of Toronto, Toronto, ON, Canada.

He is presently a seminarian at The Oratory of St. Philip Neri in Toronto.

Mark A. Tilston received the B.A.Sc. degree in 1974, the M.Eng. degree in 1983, and the Ph.D. degree in 1989, all in electrical engineering from the University of Toronto, Toronto, ON, Canada.

From 1974 to 1981 he worked as a television and radio broadcasting consultant with Elder Engineering Inc. in King City, ON. Since then, he has continued to work in that field under his own company, while concurrently working as a research assistant in numerical electromagnetic analysis at the University of Toronto. He has a special interest in the prediction of antenna pattern distortion due to the antenna environment.

Keith G. Balmain (S'56–M'63–F'87) was born in London, ON, Canada, on August 7, 1933. He received the B.A.Sc. degree in engineering physics from the University of Toronto, Toronto, ON, Canada, in 1957, and the M.S. and Ph.D. degrees in electrical engineering from the University of Illinois, Urbana, in 1959 and 1963, respectively.

He was an Assistant Professor in Electrical Engineering at the University of Illinois, associated primarily with the Aeronomy Laboratory, until 1966. Then he joined the Department of Electrical Engineering at the University of Toronto where he is now a Professor. He chaired the Division of Engineering Science for two and one-half years until 1987 when he became Chairman of the Research Board. His research has focused on antennas in plasma, broadband antennas, radio wave scattering from power lines and high-rise buildings, electrostatic charge accumulation and arc discharges on synchronous-orbit spacecraft, and electromagnetic compatibility.

Dr. Balmain was corecipient of the IEEE Antennas and Propagation Society Best Paper of the Year award in 1970. He coauthored the second edition of *Electromagnetic Waves and Radiating Systems*. His activities include: member of the IEEE Antenna Standards Committee and Chairman of the Subcommittee on Antennas in Physical Media (1968–1976); Canadian Chairman of the International Union of Radio Science Commission VI (1970–1973); member, IEEE APS AdCom (1973–1976); Associate Editor, *Radio Science* (1978–1980); Chairman, Technical Program Committee, 1980 IEEE APS International Symposium.